OXFORD

Human Molecular Genetics, 2017, Vol. 26, No. 2 333–343

doi: 10.1093/hmg/ddw389
Advance Access Publication Date: 20 December 2016
Original Article

ORIGINAL ARTICLE

Decreased WNT/β-catenin signalling contributes to the pathogenesis of dilated cardiomyopathy caused by mutations in the lamin a/C gene

Caroline Le Dour[1,2,†], Coline Macquart[3,†], Fusako Sera[1], Shunichi Homma[1], Gisele Bonne[3], John P. Morrow[1], Howard J. Worman[1,2,*] and Antoine Muchir[3,*]

[1]Department of Medicine, College of Physicians and Surgeons, [2]Department of Pathology and Cell Biology, College of Physicians and Surgeons, Columbia University, New York, NY, USA and [3]Sorbonne Universités, UPMC Univ Paris 06, INSERM UMRS974, CNRS FRE3617, Center for Research in Myology, Institut de Myologie, G.H. Pitié Salpêtrière, F-75651 Paris Cedex 13, France

*To whom correspondence should be addressed at: Antoine Muchir, Center of Research in Myology, UPMC-Inserm UMR974, CNRS FRE3617, Institut de Myologie, G.H. Pitie Salpetriere, F-75651 Paris Cedex 13, France. Email: a.muchir@institut-myologie.org
Howard J Worman, Department of Medicine, College of Physicians and Surgeons, Columbia Univesity, New York, NY 10032, USA. Email: hjw14@columbia.edu

Abstract

Cardiomyopathy caused by lamin A/C gene (*LMNA*) mutations (hereafter referred as *LMNA* cardiomyopathy) is characterized by cardiac conduction abnormalities and left ventricular systolic dysfunction predisposing to heart failure. Previous cardiac transcriptional profiling of *Lmna*$^{H222P/H222P}$ mouse, a small animal model of *LMNA* cardiomyopathy, suggested decreased WNT/β-catenin signalling. We confirmed decreased WNT/β-catenin signalling in the hearts of these mice by demonstrating decreased β-catenin and WNT proteins. This was correlated with increased expression of soluble Frizzled-related proteins that modulate the WNT/β-catenin signalling pathway. Hearts of *Lmna*$^{H222P/H222P}$ mice also demonstrated lowered expression of the gap junction connexin 43. Activation of WNT/β-catenin activity with 6-bromoindirubin-3'-oxime improved cardiac contractility and ameliorated intraventricular conduction defects in *Lmna*$^{H222P/H222P}$ mice, which was associated with increased expression of myocardial connexin 43. These results indicate that decreased WNT/β-catenin contributes to the pathophysiology of *LMNA* cardiomyopathy and that drugs activating β-catenin may be beneficial in affected individuals.

Introduction

Dominant mutations in the lamin A/C gene (*LMNA*), which encodes A-type nuclear lamins, cause dilated cardiomyopathy (herein referred to as *LMNA* cardiomyopathy), often associated with skeletal myopathy such as Emery-Dreifuss muscular dystrophy (1,2). *LMNA* cardiomyopathy is characterized by early conduction defects, impaired myocardial contractility and ventricular dilation, eventually causing heart failure (3–5). It has a more aggressive course than other inherited dilated cardiomyopathies due to the high incidence of heart block and ventricular arrhythmias (5). While sudden death from arrhythmias may be prevented by implantation of a pacemaker and/or defibrillator, the progressive heart failure eventually becomes resistant to treatment and heart transplantation is often the only therapeutic option (4).

To decipher mechanistic events underlying the pathogenesis of *LMNA* cardiomyopathy, we have studied *Lmna*$^{H222P/H222P}$

[†]Caroline Le Dour and Coline Macquart contributed equally to this article.
Received: September 2, 2016. **Revised:** October 21, 2016. **Accepted:** November 7, 2016

mice, which recapitulate the cardiac pathology that occurs in human subjects. These mice develop left ventricular dilatation and conduction defects in adulthood (6). Despite normal heart histology and the absence of left ventricular dilatation at early ages, cardiac transcriptional profiling has identified alterations in several cellular signalling pathways, including WNT/β-catenin (7,8).

WNT proteins are a family of secreted cysteine-rich glycoproteins implicated in a variety of cellular processes, including proliferation, differentiation, apoptosis, polarity, and senescence (9,10). There are 19 human *WNT* genes, which encode proteins that have been grouped into two classes: those in the canonical and non-canonical WNT pathways. In the canonical WNT signalling cascade, the expression level of β-catenin, the key effector functioning as a transcriptional co-activator, is critical for target gene expression. In the absence of WNT ligand, β-catenin is captured by the scaffold protein Axin, which facilitates its phosphorylation by glycogen synthase kinase 3-β (GSK3-β) in a destruction complex. E3-ubiquitin ligase β-TrCP then catalyzes the ubiquitination of phosphorylated β-catenin, which is subsequently rapidly degraded by the proteasome. Upon WNT ligand binding to the Frizzled and low-density lipoprotein receptor 5/6 complex, the β-catenin destruction complex becomes dysfunctional by a mechanism that is not fully understood. As a result, the newly synthesized β-catenin accumulates in the cytosol, translocates to the nucleus and forms a complex with transcription factor TCF/LEF, leading to activation of target genes.

Frizzled-related proteins and Dickkopfs are modulators of WNT/β-catenin signalling. These proteins have been shown to play a role in various cardiac pathophysiological processes (11–13). Given the alterations of WNT/β-catenin signalling in hearts of *Lmna*$^{H222P/H222P}$ mice suggested by transcriptional profiling (7,8), we explored the potential involvement of this pathway in the pathophysiology of *LMNA* cardiomyopathy.

Results

The canonical WNT/β-catenin signalling pathway is impaired in *LMNA* cardiomyopathy

Lmna$^{H222P/H222P}$ mice develop cardiomyopathy that recapitulates human *LMNA* cardiomyopathy (6). For these experiments, we reconfirmed that male *Lmna*$^{H222P/H222P}$ mice develop decreased left ventricular fractional shortening (Supplementary Material Fig. S1A,) and first degree heart block (Supplementary Material, Fig. S1B) starting at approximately 3 months and progressing to approximately 6 months of age, which is their median survival. Female *Lmna*$^{H222P/H222P}$ mice develop signs and symptoms at significantly later ages (6). We therefore evaluated cardiac expression of total β-catenin and its active form (non-phosphorylated Ser33/37/Thr41) in male *Lmna*$^{H222P/H222P}$ mice. Immunoblotting of heart lysates from 3 month-old and 6 month-old *Lmna*$^{H222P/H222P}$ mice demonstrated a decrease in both total and active forms of β-catenin compared to wild type mice (Fig. 1A). Given that β-catenin expression was lowered in hearts from *Lmna*$^{H222P/H222P}$ mice, we next assessed the canonical WNT/β-catenin signalling activity. We observed significantly decreased expression of WNT1, and WNT10b in hearts from 6 month-old *Lmna*$^{H222P/H222P}$ mice compared to wild type mice (Fig. 1B). We next showed that β-catenin expression was significantly lowered in isolated cardiomyocytes from 6-month old *Lmna*$^{H222P/H222P}$ mice compared to wild type mice (Fig. 1C). We also analysed left ventricle tissue from three human subjects with *LMNA* cardiomyopathy obtained after cardiac transplantation. Immunoblotting using antibody against total β-catenin showed decreases in this protein in heart tissue of the patients with *LMNA* mutations compared with controls (Fig. 1D). These results demonstrated decreased WNT/β-catenin signalling in hearts of *Lmna*$^{H222P/H222P}$ mice and human subjects with *LMNA* cardiomyopathy.

Increased expression of soluble frizzled-related proteins modulate the WNT/β-catenin signalling pathway in *LMNA* cardiomyopathy

Soluble Frizzled-related proteins are inhibitors of WNT/β-catenin signalling and interact with WNT proteins. We measured the expression of genes encoding members of soluble Frizzled-related protein family (*sFrp1*, *sFrp2*, *Frzb*) and Dickkopf-related protein 3 (*Dkk3*). Compared to wild type mice, 3-month old *Lmna*$^{H222P/H222P}$ mice exhibited significantly increased cardiac *sFrp1* and *Frzb* expression as well increased cardiac *Dkk3* expression (Fig. 2A). At 6 months of age, *Lmna*$^{H222P/H222P}$ mice exhibited significantly increased cardiac *sFrp1* (∼ 4 fold), *sFrp2* (∼ 2.5 fold) and *Frzb* (∼ 3 fold) mRNA expression as well increased cardiac *Dkk3* (∼ 17 fold) mRNA expression (Fig. 2A). We confirmed that the expression of sFRP1 protein was increased in hearts from 6-month old *Lmna*$^{H222P/H222P}$ mice compared to wild type mice (Fig. 2B). The expression of Dkk3 protein was similarly increased in heart tissues from subjects with *LMNA* cardiomyopathy (Fig. 2C). These data suggested that activation of extracellular inhibitors could trigger the inhibition of cardiac WNT/β-catenin signalling in *LMNA* cardiomyopathy.

Altered gap junction structure in *LMNA* cardiomyopathy

β-catenin is also located in intercalated discs (ICD). This cellular junction is a tightly regulated part of cardiomyocytes and composed of desmosomes, adherens junctions and gap junctions. Therefore, we assessed the architecture of ICDs in *Lmna*$^{H222P/H222P}$ mice. Immunofluorescence microscopic analyses of specific junctional components were performed on sections of heart tissue from 3 month-old mice as well as in isolated cardiomyocytes. The localization of β-catenin, a component of adherens junctions, was not altered in *Lmna*$^{H222P/H222P}$ mice compared to wild type mice (Fig. 3A). Similarly, the localization of N-cadherin, a component of both adherens junction and desmosomes, was not altered in *Lmna*$^{H222P/H222P}$ mice (Fig. 3B). Because of the cardiac conduction abnormalities that occur in *LMNA* cardiomyopathy, we examined the localization and expression of connexin 43, a central protein component of myocardial gap junctions. We observed decreased connexin 43 expression by immunofluorescence microscopy (Fig. 3C) and immunohistochemistry (Fig. 3D) in hearts from *Lmna*$^{H222P/H222P}$ mice compared to wild type mice. Given that the phosphorylation status of connexin 43 has been implicated in cardiovascular disease pathology (14), we next assessed the level of phosphorylated (Ser368) connexin 43 and confirmed the diminution of its expression in the hearts of 3 month-old *Lmna*$^{H222P/H222P}$ mice. Connexin 43 phosphorylation and total expression were both decreased in hearts from *Lmna*$^{H222P/H222P}$ mice compared to wild type mice (Fig. 3E). These data showed altered expression and phosphorylation of connexin 43 in *LMNA* cardiomyopathy.

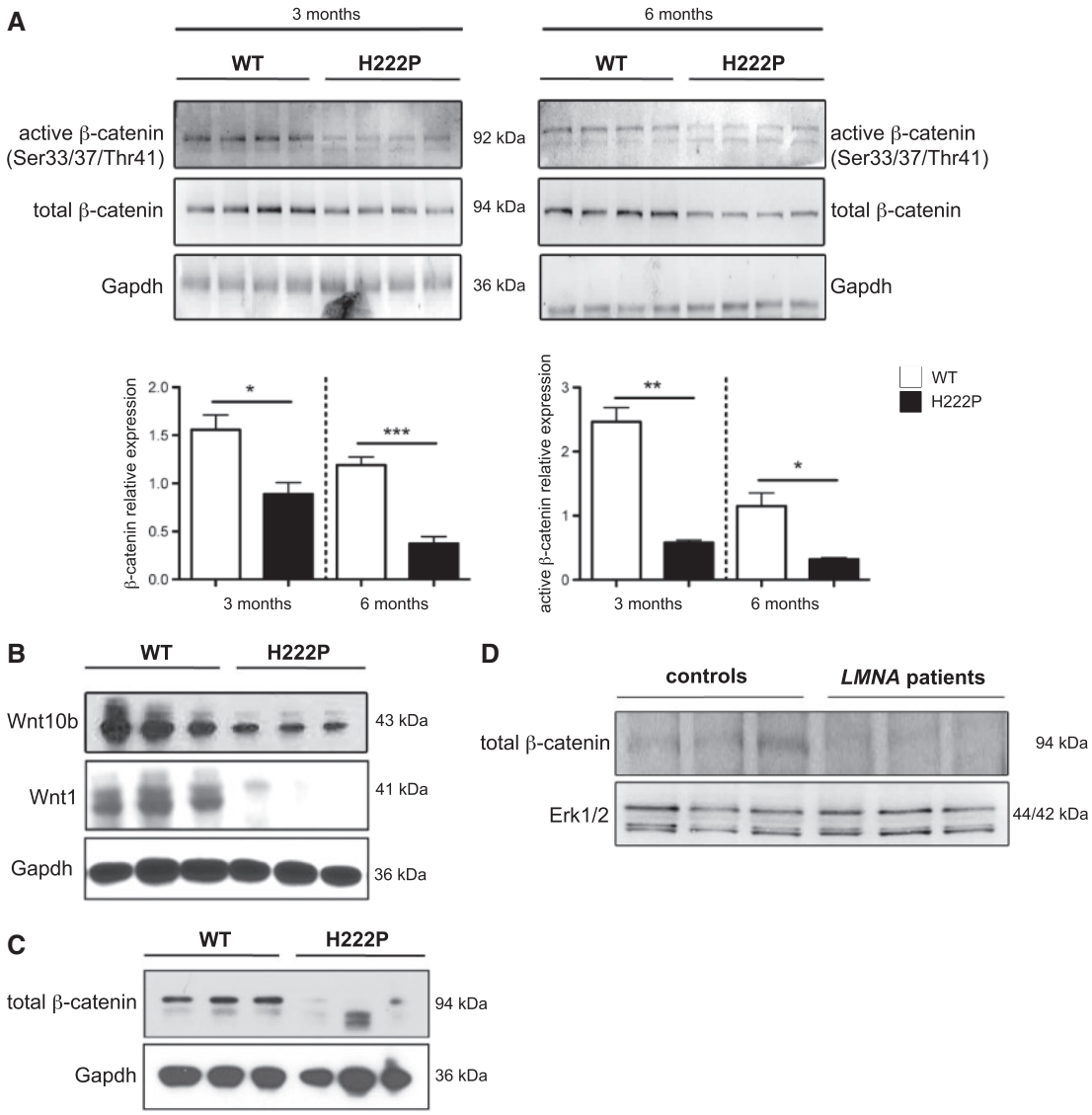

Figure 1. Altered WNT/β-catenin signalling in hearts of *Lmna*$^{H222P/H222P}$ mice and human subjects with *LMNA* cardiomyopathy. **(A)** Representative immunoblots showing active and total β-catenin expression in hearts from 3 month-old and 6 month-old male *Lmna*$^{H222P/H222P}$ (H222P) and wild type (WT) mice. Each lane contains protein extracts from a different mouse. Gapdh is the loading control. Error bars represent means ± standard errors of means ($n = 4$) for total β-catenin/gapdh and active β-catenin/total β-catenin relative expression. *$P < 0.05$, **$P < 0.005$, ***$P < 0.0005$. **(B)** Representative immunoblots showing WNT10b and WNT1, expression in hearts from 6 month-old male *Lmna* H222P mice compared to *Lmna* WT mice. Each lane contains protein extracts from a different mouse. Gapdh is the loading control. **(C)** Representative immunoblot showing total β-catenin expression in isolated cardiomyocytes from 6 month-old male *Lmna* H222P mice compared to *Lmna* WT mice. **(D)** Representative immunoblots showing total β-catenin expression in explanted hearts from control human subjects and human subjects with cardiomyopathy and *LMNA* point mutations (*LMNA* patients). Erk1/2 is the loading control (45). Migrations of molecular mass standards in kilodaltons (kDa) are indicated at the right of the blots.

Activating WNT/β-catenin signalling improves cardiac function in *LMNA*$^{H222P/H222P}$ mice

Given the altered WNT/β-catenin signalling in hearts of *Lmna*$^{H222P/H222P}$ mice, we hypothesized that increasing this pathway's activity would prevent the progression of left ventricular dysfunction and conduction defects. We therefore treated male *Lmna*$^{H222P/H222P}$ mice with daily intra-peritoneal injections of 1.25 μg/kg/day of 6-bromoindirubin-3'-oxime (BIO) (Fig. 4A). BIO is a highly potent, selective ATP-competitive inhibitor of GSK3-β that activates the WNT/β-catenin signalling (15). After 1 month of treatment starting at 4 months of age, *Lmna*$^{H222P/H222P}$ mice were analysed using echocardiography and electrocardiography and then sacrificed for biochemical and histological analyses. BIO treatment increased GSK3-β phosphorylation (inactive form) and total β-catenin in hearts of *Lmna*$^{H222P/H222P}$ mice compared to dimethyl sulfoxide (DMSO) placebo treatment (Fig. 4B). This demonstrated that BIO positively regulated WNT/β-catenin signalling. M-mode echocardiography showed that left ventricular end-diastolic and end-systolic diameters in *Lmna*$^{H222P/H222P}$ mice treated with BIO were significantly smaller and fractional shortening was significantly increased compared to placebo-treated mice (Fig. 4C; Table 1). Treating *Lmna*$^{H222P/H222P}$ mice with BIO also lead to a significant reduction of mRNA levels of *NppA* and *NppB*, genes that encode natriuretic peptide precursors that are markers for heart failure,

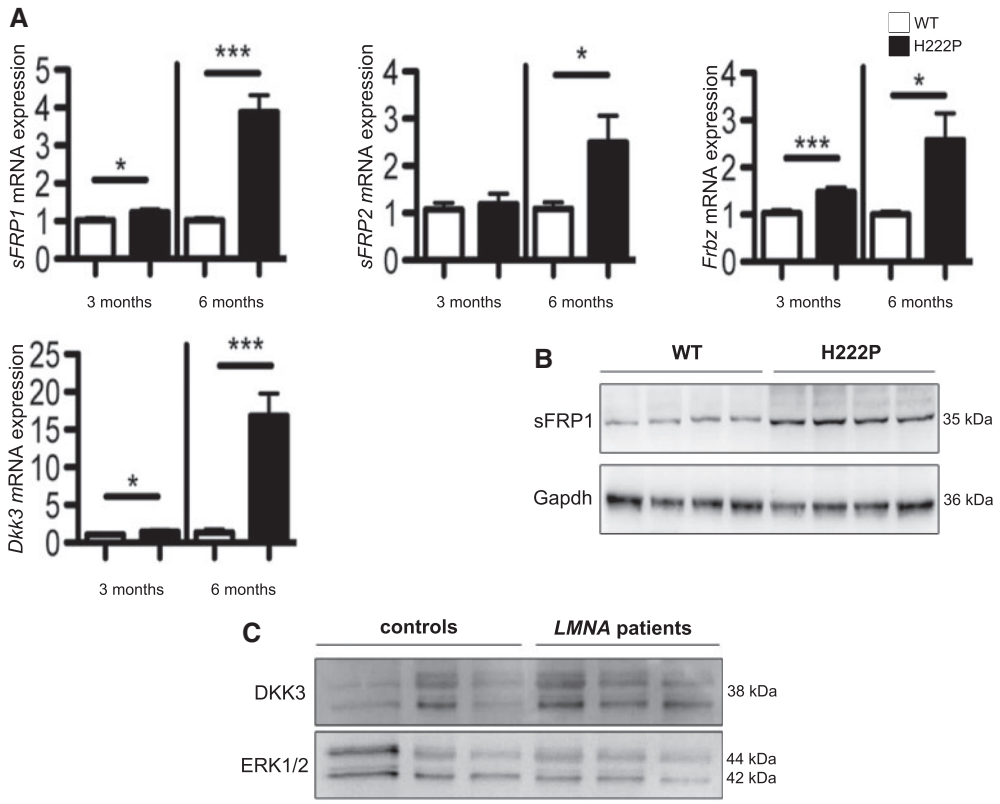

Figure 2. Increased expression of secreted antagonists of WNT/β-catenin signalling in hearts of *Lmna*$^{H222P/H222P}$ mice and human subjects with *LMNA* cardiomyopathy. **(A)** Expression of *sFRP1*, *sFRP2*, *Frbz* and *Dkk3* mRNA in hearts from 3 month-old and 6 month-old male *Lmna*$^{H222P/H222P}$ (H222P) and wild type (WT) mice. Error bars represent means ± standard errors of means ($n = 7$). $^{*}P < 0.05$, $^{***}P < 0.0005$. **(B)** Representative immunoblots showing sFRP1 expression in hearts from 6 month-old male H222P and WT mice. **(C)** Representative immunoblot showing Dkk3 expression in explanted hearts from control human subjects and human subjects with cardiomyopathy and *LMNA* point mutations (*LMNA* patients). Erk1/2 is the loading control (45). Migrations of molecular mass standards in kilodaltons (kDa) are indicated at the right of the blots in panels B and C.

as well as the mRNA levels of *Col1a1*, encoding type I collagen of the extracellular matrix (Supplementary Material, Fig. S2). The prolonged QRS interval, but not PR interval, was also significantly decreased in BIO-treated *Lmna*$^{H222P/H222P}$ mice compared to DMSO-treated mice (Fig. 4D). Treating *Lmna*$^{H222P/H222P}$ mice with increased concentrations of BIO (2.5 or 5 μg/kg, daily) did not improve the left ventricular diameters and fractional shortening (Supplementary Material, Fig. S3), suggesting a therapeutic window.

The QRS interval represents the time taken for the excitatory impulse to propagate throughout the ventricles, which is partly determined by the resistance of the intercellular connections between myocytes (16). Decreased expression of connexin 43 is associated with intraventricular conduction slowing and QRS prolongation (17–19). BIO treatment of *Lmna*$^{H222P/H222P}$ mice lead to increased expression of cardiac connexin 43, which occurs in parallel with re-expression β-catenin and WNT-1 (Fig. 5A). We confirmed this re-expression of connexin 43 by immunohistochemistry on heart from BIO-treated *Lmna*$^{H222P/H222P}$ mice compared to DMSO-treated mice (Fig. 5B). Given that correct localization of connexin 43 at gap junctions is important for myocyte-myocyte junctions and functions, we hypothesized that BIO treatment improves intraventricular conduction by normalizing expression of connexin 43 in hearts of *Lmna*$^{H222P/H222P}$ mice. To confirm that WNT/β-catenin signalling can modulate the expression of connexin 43, we treated C2C12 cells with BIO. Immunoblot analysis of cellular protein extracts showed that treatment with BIO compared to DMSO lead to an increase of connexin 43 expression concurrent with increased β-catenin signalling (Fig. 5C). Conversely, C2C12 cells treated with IWP2 or LGK974, which inhibit WNT/β-catenin signalling, showed decreased connexin 43 expression compared to DMSO-treated cells (Fig. 5D). These results demonstrated that WNT/β-catenin signalling triggers the expression of connexin 43, which is expressed at abnormally low levels in *LMNA* cardiomyopathy.

Discussion

Our findings suggest a physiological role for A-type lamins as a modifier of WNT/β-catenin signalling in the heart. This is consistent with work from Hernandez and colleagues that showed deficient WNT/β-catenin signalling activity in *Lmna*$^{L530P/530P}$ mice (20), a small animal model for premature ageing with cardiac defects (21). Some evidence suggests that WNT/β-catenin signalling is regulated by emerin, another protein of the inner nuclear membrane, which interacts with A-type lamins (22–24). Mutations in *EMD*, the gene encoding emerin, also cause dilated cardiomyopathy (25). Interaction of β-catenin with emerin might inhibit TCF/LEF-dependent transcription by restriction access of β-catenin to the nucleus. A variant of nesprin 2, a protein of the Linker of Nucleoskeleton and Cytoskeleton (LINC) complex that physically couples the cytoplasm and the nucleoplasm, has also been shown to anchor β-catenin at cell-cell junctions and negatively regulate WNT/β-catenin signalling (26). Nesprins may also be involved in the pathogenesis of dilated cardiomyopathy (27–29). Hence, A-type lamins, emerin

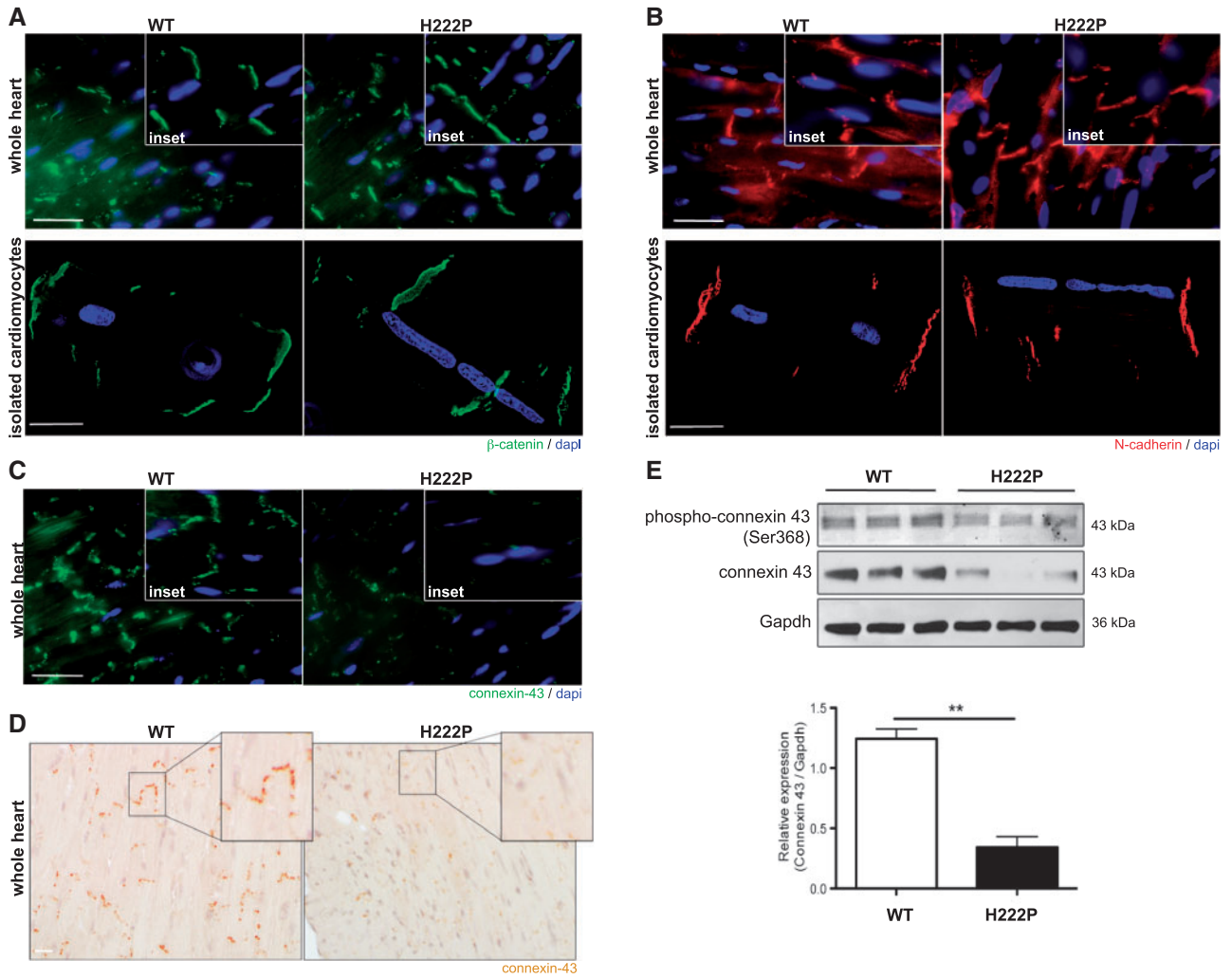

Figure 3. Decreased expression of connexin 43 in hearts of *Lmna*$^{H222P/H222P}$ mice. **(A)** Micrographs showing β-catenin labelling (green) in heart and isolated cardiomyocytes from male *Lmna*$^{H222P/H222P}$ (H222P) and wild type (WT) mice. Nuclei are counter-stained blue with 4′,6-diamidino-2-phenylindole (dapi). Scale bar, 25 μm. Insets are a representative area. **(B)** Micrographs showing N-cadherin labelling (red) in heart and isolated cardiomyocytes from H222P and WT mice. Nuclei are counter-stained with dapi. Scale bar, 25 μm. Insets are a representative area. **(C)** Micrographs showing connexin 43 labelling (green) in heart from male H222P mice and WT mice. Nuclei are counter-stained with dapi. Scale bar, 25 μm. Insets are a representative area. **(D)** Immunohistochemical labelling for connexin 43 in heart from H222P and WT mice. Scale bar, 25 μm. Insets are a representative area. (E) Representative immunoblot showing phospho-connexin 43 (ser368) and total connexin 43 expression in hearts from 6 month-old male H222P and WT mice. Migrations of molecular mass standards in kilodaltons (kDa) are indicated at the right of the blots. The bar graph shows connexin 43 relative expression compared to Gapdh (means ± standard errors of means) in hearts from WT ($n = 3$) and H222P ($n = 3$) mice. **$P < 0.005$.

and nesprins may form a complex that modulates, at least to some extent, similar cellular signalling pathways that are involved in the pathogenesis of dilated cardiomyopathy.

Activation of WNT/β-catenin signalling has been reported to be involved in cardiac hypertrophy (30). There is increasing evidence that WNT/β-catenin signalling is also involved in cardiac remodelling and the progression to heart failure. We observed an up-regulation of soluble modulators of WNT/β-catenin signalling in hearts of *Lmna*$^{H222P/H222P}$ mice and human subjects with *LMNA* cardiomyopathy. Enhanced expression of Frizzled transcripts has been reported in several heart diseases and cardiomyopathies (30). Therefore, we can speculate that the up-regulation of soluble modulators of WNT/β-catenin signalling could be a consequence of molecular defects leading to cardiomyopathy and heart failure, with no specificity to *LMNA* cardiomyopathy. The mRNA levels of sFRP3 and sFRP4 are elevated in failing ventricles compared with control donor hearts (29). However, this finding contradicts other work showing that there is a decreased level of sFRPs in heart in an animal model of cardiac failure and in human cardiomyopathies (31). Accordingly, administration of sFRP2 improves cardiac function in a rat model of myocardial infarction (32). Similarly, overexpression of sFRP1 improves infarct healing and cardiac function in mice (11). This effect appears to occur by altering type I procollagen processing by inhibiting bone morphogenic protein 1 in primary cardiac fibroblasts and therefore reducing fibrosis. Our observation showing Dkk3 overexpression in hearts from *Lmna*$^{H222P/H222P}$ mice is in contrast to other published work showing that Dkk3 attenuated pressure overload-induced cardiac remodelling (12) and protected against cardiac dysfunction and ventricular remodelling following myocardial infarction (13). However, the pathogenic processes leading to cardiac dysfunction after infarction and in primary cardiomyopathies are likely to be very different.

Several converging lines of evidence have suggested that the effects of WNT/β-catenin signalling may result in part via

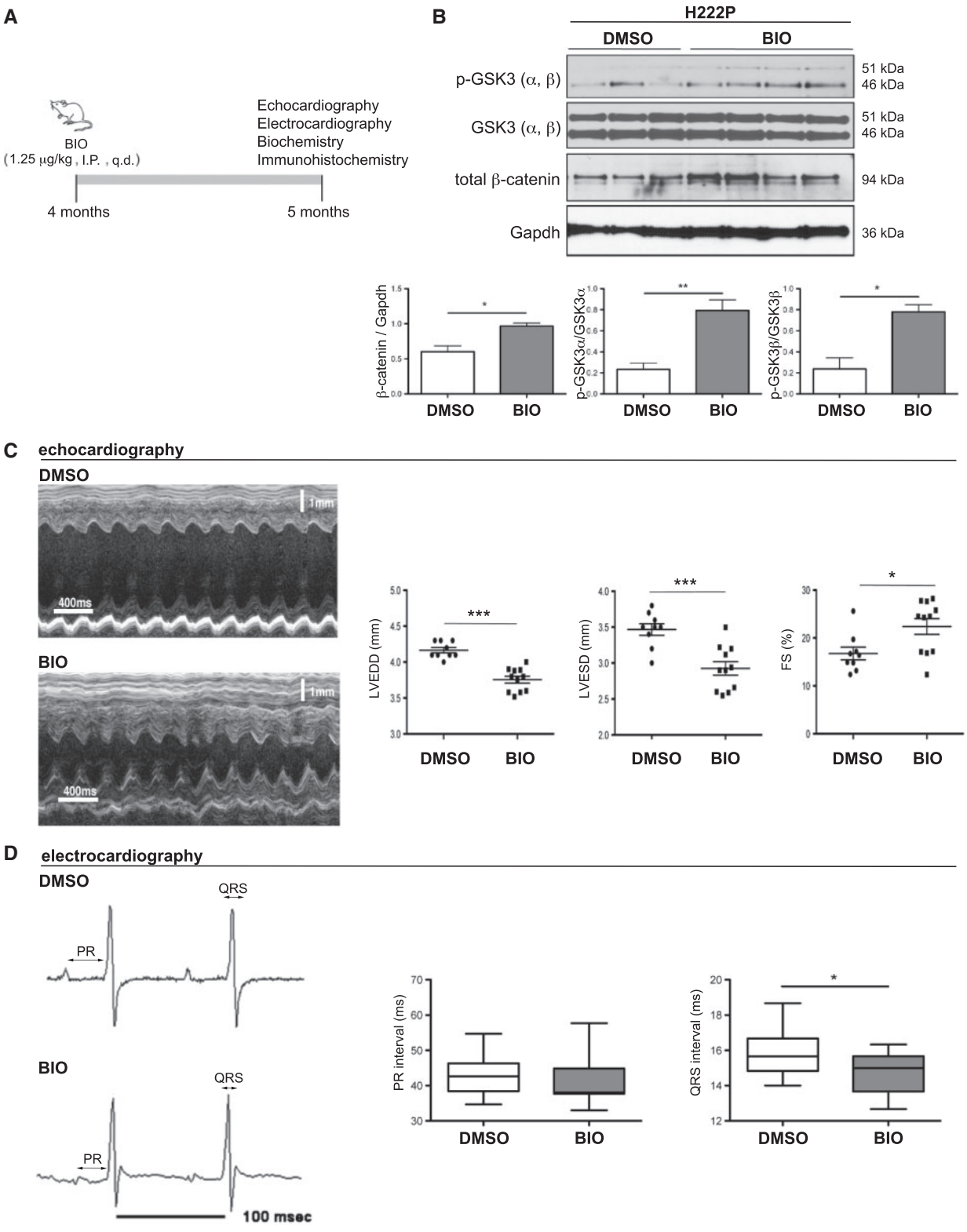

Figure 4. Activation of WNT/β-catenin signalling using BIO improves left ventricular function and intraventricular conduction in *Lmna*$^{H222P/H222P}$ mice. **(A)** Schematic representation of the treatment protocol of *Lmna*$^{H222P/H222P}$ (H222P) with BIO. I.P., intra-peritoneal; q.d., daily. **(B)** Representative immunoblots showing phospho-GSK3, total GSK3 and total β-catenin expression in hearts from 6 month-old male H222P mice treated with DMSO placebo or BIO (1.25 µg/kg/daily). Migrations of molecular mass standards in kilodaltons (kDa) are indicated at the right of the blots. Error bars represent means ± standard errors of means for total β-catenin/gapdh, p – GSK3/total GSK3 and p – GSK3/total GSK3 relative expression in 20-week-old male H222P mice treated with BIO ($n = 4$) or DMSO ($n = 3$). $^{*}P < 0.05$, $^{**}P < 0.005$. **(C)** Representative M-mode transthoracic echocardiographic tracings from 20-week-old male H222P mice treated with DMSO or BIO. Graphs show mean left ventricular end-diastolic diameter (LVEDD), left ventricular end-systolic diameter (LVESD), and left ventricular fractional shortening (FS) in 20-week-old male H222P mice treated with BIO ($n = 5$) or DMSO ($n = 8$). Values for each individual mouse as well as means ± standard errors of means are shown. $^{*}P < 0.05$, $^{***}P < 0.0005$. **(D)** Representative electrocardiogram tracings from 20-week-old H222P mice treated with DMSO or BIO. Graphs showing mean PR and QRS intervals in 20-week-old H222P mice treated with BIO ($n = 5$) or DMSO ($n = 8$). Data are represented as means ± standard errors of means. Values are shown as 25th to 75th percentiles of data values. The line in the middle is the median. Whiskers (Tukey method) extend down to the minimum value and up to the maximum value. $^{*}P < 0.05$.

Table 1. Echocardiographic parameters for male wild type (WT) and *Lmna*$^{H222P/H222P}$ (H222P) mice treated with either BIO or DMSO

Genotype	Treatment	*n*	Heart rate (bpm)	LVEDD (mm)	LVESD (mm)	FS (%)
WT	none	5	534.8 ± 31.8	3.2 ± 0.5	1.8 ± 0.3	45.7 ± 1.5
H222P	DMSO	8	501.7 ± 2.9	4.2 ± 0.1	3.5 ± 0.2	15.7 ± 2.4
H222P	BIO	5	496.3 ± 9.3	3.6 ± 0.2***	2.8 ± 0.3***	24.5 ± 5.2**

LVEDD, left ventricular end-diastolic diameter; LVESD, left ventricular end-systolic diameter; FS, fractional shortening. Values are means ± standard errors of means.
**$P < 0.005$, ***$P < 0.0005$ between DMSO-treated and BIO-treated H222P mice.

modulation of gap junction channel activity. In response to WNT signalling, β-catenin interacts with the gene encoding connexin 43 to increase its transcription and also appears to interact with connexin 43, likely as part of a complex with the ICD (33). Whether this interaction is direct or requires other components of cell junctions remains to be determined. Several groups have documented downregulation or abnormal localization of connexins in experimental and human cardiomyopathies (34,35). This process, referred to as gap junction remodelling, is thought to predispose to cardiac conduction alterations. The robust response of connexin 43 expression to WNT/β-catenin signalling (33,36,37) suggests that alteration in WNT/β-catenin signalling might influence gap junction channel gene expression in the heart. This is supported by recent data showing that LRP6 deficiency disrupts gap junction formation and function (38). Our results showing a concordant decrease in β-catenin and connexin 43 levels in hearts from *Lmna*$^{H222P/H222P}$ mice are consistent with this hypothesis.

We have shown that the pharmacological activation of WNT/β-catenin signalling using a GSK3-β inhibitor induces connexin 43 expression and improves left ventricular dysfunction in *Lmna*$^{H222P/H222P}$ mice. Identified in the late 1970s as a protein kinase that inactivates glycogen synthase, GSK3 became a drug target when its role in insulin signal transduction and its potential importance for Alzheimer disease started to emerge (39). Several potent inhibitors of GSK3 have been identified with therapeutic potential (40). However, long-term use of GSK3 inhibitors may have potential problems. GSK3 inhibitors might be expected to mimic the WNT/β-catenin signalling and therefore could be potentially carcinogenic (41). Nonetheless, lithium, which is a potent GSK3 inhibitors, have been used to treat bipolar disorder, and their long-term use is not known to be associated with an increased risk of cancer (42). Careful adjustment of WNT/β-catenin signalling activity in *LMNA* cardiomyopathy using small molecule activators might therefore have beneficial effects in humans with *LMNA* cardiomyopathy. We have previously shown that pharmacological blockade of other signalling cascades - ERK1/2 (43–45), AKT/mTOR (46), TGF-β (47), CTGF (47), JNK (48), p38α (8) - also has beneficial effects on left ventricular function in *Lmna*$^{H222P/H222P}$ mice. Future studies could be designed to assess the therapeutic benefit of blocking combinations of these signalling pathways in *LMNA* cardiomyopathy.

Materials and Methods

Mice

Lmna$^{H222P/H222P}$ mice were bred and genotyped as previously described. Mice were fed chow and housed in a disease-free barrier facility with 12h/12h light/dark cycles. The Institutional Animal Care and Use Committee at Columbia University Medical Center approved the use of animals and the study protocols.

Isolation of mouse cardiomyocytes

Wild type and *Lmna*$^{H222P/H222P}$ mice (16 weeks of age) were anaesthetized with pentofurane. Ventricular cardiomyocytes were isolated as described in the Alliance for Cellular Signaling procedure protocol PP00000125 (http://www.signaling-gateway.org/data/ProtocolLinks.html). Briefly, hearts were removed and the aorta cannulated. After Ca^{2+}-free buffer was perfused for two minutes, 0.25 mg/ml collagenase I/II (Roche) solution was perfused through the coronary arteries for 6 min with 12.5 μM Ca^{2+}. Left ventricular tissue was teased apart and pipetted to release individual cells. After enzymatic dispersion, Ca^{2+} concentration in the buffer containing bovine serum albumin was elevated in three steps up to 500 μM.

Human tissue samples

Sections of explanted hearts from human subjects with *LMNA* mutations were obtained from Myobank-AFM of l'Institut de Myologie. The subjects were a 23 year-old man with cardiomyopathy associated with muscular dystrophy and *LMNA* delK61 mutation, a 47 year-old woman with cardiomyopathy and *LMNA* R60G mutation and from a 62 year-old woman with cardiomyopathy associated with muscular dystrophy and *LMNA* c.IVS9 + 1g sup a mutation. Control human heart samples were obtained from the National Disease Research Interchange from a 57 year-old man with an intracranial bleed and a 15 year-old woman who died of a drug overdose. All tissue samples were obtained with appropriate approvals and consent from l'Institut de Myologie and the National Disease Research Interchange and provided without patient identifiers.

Cell culture and reagents

C2C12 mouse myoblasts (ATCC) were maintained in DMEM supplemented with 10% Fetal Bovine Serum. Cells were incubated with BIO (10 μM) for 24 h, IWP2 (20 μM) for 24 h and LGK974 (8 μM) for 24 h.

Quantitative real-time RT-PCR analysis

Total RNA was extracted (Rneasy isolation kit, Qiagen) and cDNA was synthesized using Superscript first strand synthesis system according to the manufacturer's instructions (Invitrogen). For each replicate in each experiment, RNA from tissue samples of different animals was used. Primers were designed corresponding to mouse RNA sequences using Primer3 (http://frodo.wi.mit.edu/cgi-bin/primer3/primer3_www.cgi). Real-time quantitative RT-PCR reactions contained HotStart-IT SYBR green qPCR Master Mix (Affymetrix), 200 nM of each primer and 0.2 μl of template in a 25 μl reaction volume. Amplification was carried out using the ABI 7300 Real-Time PCR

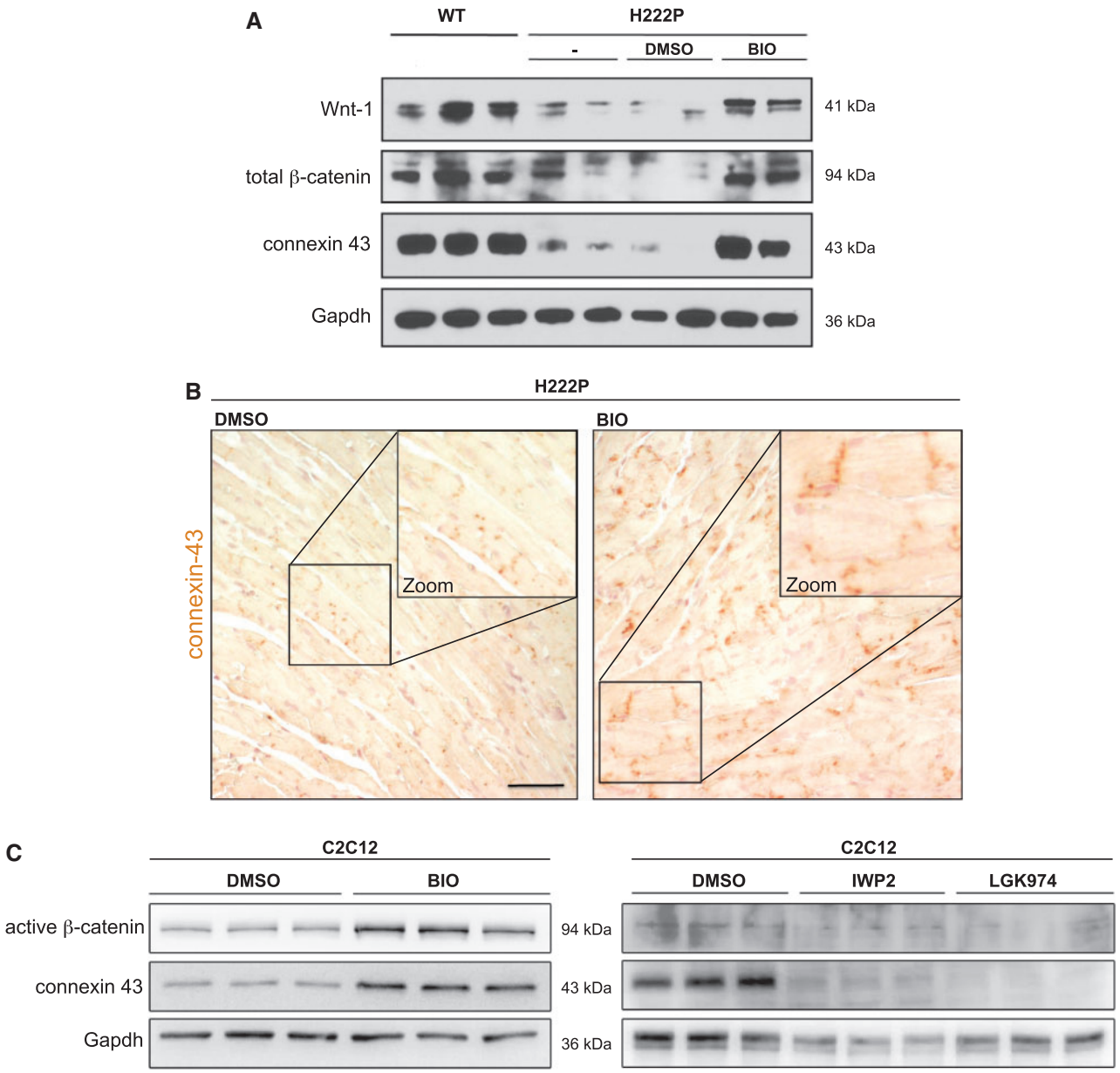

Figure 5. Expression and localization of connexin 43 are under WNT/β-catenin signalling regulation in hearts from *Lmna*$^{H222P/H222P}$ mice and cultured C2C12 cells. **(A)** Representative immunoblots showing WNT-1, total β-catenin and connexin 43 expression in hearts from 20-week-old male wild type (WT) and *Lmna*$^{H222P/H222P}$ (H222P) mice untreated (-), treated with BIO or with DMSO. **(B)** Immunohistochemistry for connexin 43 labelling in hearts from H222P mice treated with BIO or with DMSO. Scale bar, 50 μm. **(C)** Representative immunoblot showing connexin 43 and active β-catenin expression in C2C12 cells treated with BIO to activate Wnt/β-catenin signalling, or IWP2 and LGK974 to inhibit Wnt/β-catenin signalling. Migrations of molecular mass standards in kilodaltons (kDa) are indicated between the blots.

System (Applied Biosystems). Relative levels of mRNA expression were calculated using the $\Delta\Delta C_T$ method. Individual expression values were normalized by comparison to *Gapdh* mRNA.

Protein extraction and immunoblotting

Human or mouse heart tissue was homogenized in sample extraction buffer (Cell Signalling) as previously described (8). Extracted proteins were separated by SDS-polyacrylamide gel electrophoresis, transferred to nitrocellulose membranes and blotted with primary antibodies against β-catenin (No ab16051, Abcam), non-phosphorylated (active) β-catenin (No 8814, Cell Signalling), WNT1 (No sc-5630, Santa Cruz Biotechnologies), WNT10b (No sc-25524, Santa Cruz Biotechnologies), sFRP1 (No ab4193, Abcam), DKK3 (No sc-14956, Santa Cruz Biotechnologies), connexin 43 (No 3512, Cell Signalling), phosphorylated (ser368) connexin 43 (No 3511, Cell Signalling) and Gapdh (No sc-25778, Santa Cruz Biotechnologies). Secondary antibodies were horseradish peroxidate–conjugated (GE Healthcare). Recognized proteins were visualized by enhanced chemiluminescence (GE Healthcare).

Immunofluorescence microscopy

For immunofluorescence microscopy, frozen tissues were cut in 8 μm-thick sections. Cryosections were fixed (15 min, 4%

paraformaldehyde in phosphate-buffered saline [PBS] at room temperature), permeabilized (10 min, 0.5% Triton X-100 in PBS) and blocked (1 h, PBS with 0.3% Triton X-100, 5% bovine serum albumin). Sections were incubated with primary antibodies against β-catenin (No ab16051, Abcam), connexin 43 (No ab11370, Abcam) and N-cadherin (No 33-3900, Invitrogen) (overnight, 4 °C, in PBS with 0.1% Triton X-100 and 1% bovine serum albumin) and washed in PBS. The sections were then incubated for 1 h with secondary antibodies. Sections were washed with PBS and slides were mounted in Vectashield mounting medium containing 4′,6-diamidino-2-phenylindole (Vector Laboratories).

Immunohistochemistry

Sections of heart tissue were fixed (24 h, 4% paraformaldehyde in PBS, pH 7.4 at 4 °C), dehydrated (EtOH 80%, 95%, and 100%, sequentially), embedded in paraffin and sectioned at 5 μm. Sections were incubated with primary antibodies against mouse anti-connexin 43 (No ab11370, Abcam).

Mouse treatment protocols

BIO was dissolved in DMSO and delivered at doses of 1.25, 2.5 or 5 μg/kg, daily. BIO and DMSO were administered by intraperitoneal injections starting when the mice were 16 weeks of age and continued until 20 weeks of age.

Thansthoracic echocardiography

Mice were anaesthetized with 1.5% isoflurane in O_2 and placed on a heating pad (37 °C). Echocardiography was performed using a Visualsonics Vevo 770 ultrasound with a 30 MHz transducer applied to the chest wall. Cardiac ventricular dimensions and fractional shortening were measured in 2D mode and M-mode 3 times for the number of animals indicated.

Electrocardiography

Electrocardiograms were recorded from mice sedated with low-dose inhaled isoflurane using the standard four limb leads and a B08 amplifier (Emka Technologies) with minimal filtering. Waveforms were recorded using Iox Software v1.8.9.18 and intervals were measured manually with ECG Auto v1.5.12.50, using the average of three representative consecutive beats. The electrocardiographer was blinded to mouse genotype.

Statistics

Values for real-time quantitative RT-PCR were compared using an unpaired Student *t*-test. Comparisons of echocardiographic parameters between BIO-treated and DMSO-treated $Lmna^{H222P/H222P}$ mice were performed using a Welch *t*-test; to validate these results, a non-parametric test (Mann-Whitney) was performed and concordance checked. Statistical analyses were performed using GraphPad Prism software.

Supplementary Material

Supplementary Material is available at *HMG* online.

Conflict of Interest statement. None declared.

Funding

This work was is supported by the National Institutes of Health [AR048997 to H.J.W.], a grant from the Association Française contre les Myopathies to C.L.D. and from the Institut National de la Sante et de la Recherche Médicale; the Université Pierre et Marie Curie-Paris 6, the Centre National de la Recherche Scientifique and the Association Française contre les Myopathies to A.M. The content is solely the responsibility of the authors and does not necessarily represent the official views of the National Institutes of Health.

References

1. Bonne, G., Di Barletta, M.R., Varnous, S., Becane, H.M., Hammouda, E.H., Merlini, L., Muntoni, F., Greenberg, C.R., Gary, F., Urtizberea, J.A., *et al.* (1999) Mutations in the gene encoding lamin A/C cause autosomal dominant Emery-Dreifuss muscular dystrophy. *Nat. Genet.*, **21**, 285–288.
2. Fatkin, D., MacRae, C., Sasaki, T., Wolff, M.R., Porcu, M., Frenneaux, M., Atherton, J., Vidaillet, H.J., Jr, Spudich, S., *et al.* (1999) Missense mutations in the rod domain of the lamin A/C gene as causes of dilated cardiomyopathy and conduction-system disease. *N. Engl. J. Med.*, **341**, 1715–1724.
3. Meune, C., Van Berlo, J.H., Anselme, F., Bonne, P., Pinto, Y.M. and Duboc, D. (2006) Primary prevention of sudden death in patients with lamin A/C gene mutations. *N. Engl. J. Med.*, **354**, 209–210.
4. Ben Yaou, R., Gueneau, L., Demay, L., Stora, S., Chikhaoui, K., Richard, P. and Bonne, G. (2006) Heart involvement in lamin A/C related diseases. *Arch. Mal. Coeur Vaiss.*, **99**, 848–855.
5. Lu, J.T., Muchir, A., Nagy, P.L. and Worman, H.J. (2011) *LMNA* cardiomyopathy: cell biology and genetics meet clinical medicine. *Dis. Model. Mech.*, **4**, 562–568.
6. Arimura, T., Helbling-Leclerc, A., Massart, C., Varnous, S., Niel, F., Lacène, E., Fromes, Y., Toussaint, M., Mura, A.M., Keller, D.I., *et al.* (2005) Mouse model carrying H222P-Lmna mutation develops muscular dystrophyand dilated cardiomyopathy similar to human striated muscle laminopathies. *Hum. Mol. Genet.*, **14**, 155–169.
7. Muchir, A., Pavlidis, P., Decostre, V., Herron, A.J., Arimura, T., Bonne, G. and Worman, H.J. (2007) Activation of MAPK Pathway Links LMNA Mutations to Cardiomyopathy in Emery-Dreifuss Muscular Dystrophy. *J. Clin. Invest.*, **117**, 1282–1293.
8. Muchir, A., Wu, W., Choi, J.C., Iwata, S., Morrow, J., Homma, S. and Worman, H.J. (2012) Abnormal p38a mitogen-activated protein kinase signalling in dilated cardiomyopathy caused by lamin A/C gene mutation. *Hum. Mol. Genet.*, **21**, 4325–4333.
9. Moon, R.T., Kohn, A.D., De Ferrari, G.V. and Kaykas, A. (2004) WNT and beta-catenin signalling: diseases and therapies. *Nat. Rev. Genet.*, **5**, 691–701.
10. Reya, T. and Clevers, H. (2005) Wnt signaling in stem cells and cancer. *Nature*, **6**, 314–322.
11. Barandon, L., Couffinhal, T., Ezan, J., Dufourcq, P., Costet, P., Alzieu, P., Leroux, L., Moreau, C., Dare, D. and Duplàa, C. (2003) Reduction of infarct size and prevention of cardiac rupture in transgenic mice overexpressing FrzA. *Circulation*, **108**, 2282–2289.
12. Zhang, Y., Liu, Y., Zhu, X.H., Zhang, X.D., Jiang, D.S., Bian, Z.Y., Zhang, X.F., Chen, K., Wei, X., Gao, L., *et al.* (2014)

Dickkopf-3 attenuates pressure overload-induced cardiac remodeling. *Cardiovasc. Res.*, **102**, 35–45.
13. Bao, M.W., Cai, Z., Zhang, X.J., Li, L., Liu, X., Wan, N., Hu, G., Wan, F., Zhang, R., Zhu, X., *et al.* (2015) Dickkopf-3 protects against cardiac dysfunction and ventricular remodeling following myocardial infarction. *Basic Res. Cardiol.*, **110**, 25–42.
14. Hatanaka, K., Kawata, H., Toyofuku, T. and Yoshida, K. (2004) Down-regulation of connexin43 in early myocardial ischemia and protective effect by ischemic preconditioning in rat hearts in vivo. *Jpn Heart J.*, **45**, 1007–1019.
15. Sato, N., Meijer, L., Skaltsounis, L., Greengard, P. and Brivanlou, A.H. (2004) Maintenance of pluripotency in human and mouse embryonic stem cells through activation of Wnt signaling by a pharmacological GSK-3-specific inhibitor. *Nat. Med.*, **10**, 55–63.
16. Rohr, S. (2004) Role of gap junctions in the propagation of the cardiac action potential. *Cardiovasc. Res.*, **62**, 309–322.
17. de Groot, J.R., Veenstra, T., Verkerk, A.O., Wilders, R., Smits, J.P., Wilms-Schopman, F.J., Wiegerinck, R.F., Bourier, J., Belterman, C.N., Coronel, R., *et al.* (2003) Conduction slowing by the gap junctional uncoupler carbenoxolone. *Cardiovasc. Res.*, **60**, 288–297.
18. Thomas, S.A., Schuessler, R.B., Berul, C.I., Beardslee, M.A., Beyer, E.C., Mendelsohn, M.E. and Saffitz, J.E. (1998) Disparate effects of deficient expression of connexin43 on atrial and ventricular conduction: evidence for chamber-specific molecular determinants of conduction. *Circulation*, **97**, 686–691.
19. Gutstein, D.E., Morley, G.E., Tamaddon, H., Vaidya, D., Schneider, M.D., Chen, J., Chien, K.R., Stuhlmann, H. and Fishman, G.I. (2001) Conduction slowing and sudden arrhythmic death in mice with cardiac-restricted inactivation of connexin43. *Circ. Res.*, **88**, 333–339.
20. Hernandez, L., Roux, K.J., Wong, E.S., Mounkes, L.C., Mutalif, R., Navasankari, R., Rai, B., Cool, S., Jeong, J.W., Wang, H., *et al.* (2010) Functional coupling between the extracellular matrix and nuclear lamina by Wnt signaling in progeria. *Dev, Cell*, **19**, 413–425.
21. Mounkes, L.C., Kozlov, S., Hermandez, L., Sullivan, T. and Stewart, C.L. (2003) A progeroid syndrome in mice is caused by defects in A-type lamins. *Nature*, **423**, 298–301.
22. Markiewicz, E., Tilgner, K., Barker, N., van de Wetering, M., Clevers, H., Dorobek, M., Hausmanova-Petrusewicz, I., Ramaekers, F.C., Broers, J.L., Blankesteijn, W.M., *et al.* (2006) The inner nuclear membrane protein emerin regulates beta-catenin activity by restricting its accumulation in the nucleus. *Embo J.*, **25**, 3275–3285.
23. Wheeler, M.A., Warley, A., Roberts, R.G., Ehler, E. and Ellis, J.A. (2010) Identification of an emerin-beta-catenin complex in the heart important for intercalated disc architecture and beta-catenin localisation. *Cell. Mol. Life Sci.*, **67**, 781–796.
24. Stubenvoll, A., Rice, M., Wietelmann, A., Wheeler, M. and Braun, T. (2015) Attenuation of Wnt/β-catenin activity reverses enhanced generation of cardiomyocytes and cardiac defects caused by the loss of emerin. *Hum. Mol. Genet.*, **24**, 802–813.
25. Bione, S., Maestrini, E., Rivella, S., Mancini, M., Regis, S., Romeo, G. and Toniol0, D. (1994) Identification of a novel X-linked gene responsible for Emery-Dreifuss muscular dystrophy. *Nat. Genet.*, **8**, 323–327.
26. Zhang, Q., Minaisah, R.-M., Ferraro, E., Li, C., Porter, L.J., Zhou, C., Gao, F., Zhang, J., Rajgor, D., Autore, F., *et al.* (2016) N-terminal nesprin-2 variants regulate β-catenin signalling. *Exp. Cell Res.*, **345**, 168–179.
27. Puckelwartz, M.J., Kessler, E.J., Kim, G., DeWitt, M.M., Zhang, Y., Earley, J.U., Depreux, F.F.S., Holaska, J., Mewborn, S.K., Pytel, P., *et al.* (2010) Nesprin-1 mutations in human and murin cardiomyopathy. *J. Mol. Cell. Cardiol.*, **48**, 600–608.
28. Banerjee, I., Zhang, J., Moore-Morris, T., Pfeiffer, E., Buchholz, K.S., Liu, A., Ouyang, K., Stroud, M.J., Gerace, L., Evans, S.M., *et al.* (2014) Targeted ablation of nesprin 1 and nesprin 2 from murine myocardium results in cardiomyopathy, altered nuclear morphology and inhibition of the biochemical gene response. *PLoS Genet.*, **10**, e1004114.
29. Schumann, H., Holtz, J., Zerkowski, H.R. and Hatzfeld, M. (2000) Expression of secreted frizzled related proteins 3 and 4 in human ventricular myocardium correlates with apoptosis related gene expression. *Cardiovasc. Res.*, **45**, 720–728.
30. Hermans, K.C.M. and Blankesteijn, W.M. (2015) Wnt signaling in cardiac disease. *Compr. Physiol.*, **5**, 1183–1209.
31. Sklepkiewicz, P., Shiomi, T., Kaur, R., Sun, J., Kwon, S., Mercer, B., Bodine, P., Schermuly, R.T., George, I., Schulze, P.C., *et al.* (2015) Loss of secreted frizzled-related protein-1 leads to deterioration of cardiac function in mice and plays a role in human cardiomyopathy. *Circ. Heart Fail.*, **8**, 362–372.
32. He, W., Zhang, L., Ni, A., Zhang, Z., Mirotsou, M., Mao, L., Pratt, R.E. and Dzau, V.J. (2010) Exogenously administered secreted frizzled related protein 2 (Sfrp2) reduces fibrosis and improves cardiac function in a rat model of myocardial infarction. *Proc. Natl. Acad. Sci. USA*, **107**, 21110–21115.
33. Van der Heyden, M.A., Rook, M.B., Hermans, M.M., Rijksen, G., Boonstra, J., Defize, L.H. and Destrée, O.H. (1998) Identification of connexin43 as a functional target fro Wnt signaling. *J Cell. Sci.*, **111**, 1741–1749.
34. Severs, N.J., Bruce, A.F., Dupont, E. and Rothery, S. (2008) Remodelling of gap junctions and connexin expression in diseased myocardium. *Cardiovasc. Res.*, **80**, 9–19.
35. Kostin, S., Rieger, M., Dammer, S., Hein, S., Richter, M., Klövekorn, W.P., Bauer, E.P. and Schaper, J. (2003) Gap junction remodeling and altered connexin43 expression in the failing human heart. *Mol. Cell. Biochem.*, **242**, 135–144.
36. Olson, D.J., Christian, J.L. and Moon, R.T. (1991) Effect of wnt-1 and related proteins on gap junctional communication in Xenopus embryos. *Science*, **252**, 1173–1176.
37. Ai, Z., Fischer, A., Spray, D.C., Brown, A.M. and Fishman, G.I. (2000) Wnt-a regulation of connexin 43 in cardiac myocytes. *J. Clin. Invest.*, **105**, 161–171.
38. Li, J., Li, C., Liang, D., Lv, F., Yuan, T., The, E., Ma, X., Wu, Y., Zhen, L., Xie, D., *et al.* (2016) LRP6 acts as a scaffold protein in cardiac gap junction assembly. *Nat. Comm.*, **7**.
39. Cohen, P. (1979) The fifteenth Colworth Medal Lecture: The hormaonal control of glycogen metabolism in mammalian muscle by multivalent phosphorylation. *Biochem. Soc. Trans.*, **7**, 459–480.
40. Cohen, P. and Goedert, M. (2004) GSK3 inhibitors: development and therapeutic potential. *Nat. Rev.*, **3**, 479–487.
41. Coghlan, M.P., Culbert, A.A., Cross, D.A., Corcoran, S.L., Yates, J.W., Pearce, N.J., Rausch, O.L., Murphy, G.J., Carter, P.S., Roxbee Cox, L., *et al.* (2000) Selective small molecule inhibitors of glycogen synthase kinase-3 modulate glycogen metabolism and gene transcription. *Chem. Biol.*, **7**, 793–803.
42. Cohen, Y., Chetrit, A., Cohen, Y., Sirota, P. and Modan, B. (1998) Cancer morbidity in psychiatric patients: influence of lithium carbonate treatment. *Med. Oncol.*, **15**, 32–36.
43. Muchir, A., Shan, J., Bonne, G., Lehnart, S.E. and Worman, H.J. (2009) Inhibition of extracellular signal-regulated kinase signaling to prevent cardiomyopathy caused by mutation in

the gene encoding A-type lamins. *Hum. Mol. Genet.*, **19**, 241–247.
44. Wu, W., Muchir, A., Shan, J., Bonne, G. and Worman, H.J. (2011) Mitogen-activated protein kinase inhibitors improve heart function and prevent fibrosis in cardiomyopathy caused by mutation in lamin A/C gene. *Circulation*, **123**, 53–61.
45. Muchir, A., Reilly, S.A., Wu, W., Iwata, S., Homma, S., Bonne, G. and Worman, H.J. (2012) Treatment with selumetinib preserves cardiac function and improves survival in cardiomyopathy caused by mutation in the lamin A/C gene. *Cardiovasc. Res.*, **93**, 311–319.
46. Choi, J.C., Muchir, A., Wu, W., Iwata, S., Homma, S., Morrow, J.P. and Worman, H.J. (2012) Temsirolimus activates autophagy and ameliorates cardiomyopathy caused by lamin A/C gene mutation. *Sc. Transl. Med.*, **4**, 144ra102.
47. Chatzifrangkeskou, M., Le Dour, C., Wu, W., Morrow, J.P., Joseph, L.C., Beuvin, M., Sera, F., Homma, S., Vignier, N., Mougenot, N., *et al.* (2016) ERK1/2 directly acts on CTGF/CCN2 expression to mediate myocardial fibrosis in cardiomyopathy caused by mutations in the lamin A/C gene. *Hum. Mol. Genet.*, **pii**, ddw090.
48. Wu, W., Shan, J., Bonne, G., Worman, H.J. and Muchir, A. (2016) Pharmacological inhibition of c-Jun N-terminal kinase signaling prevents cardiomyopathy caused by mutation in LMNA gene. *Bioch. Biophys. Acta*, **1802**, 632–638.